



## Parametric study on degradation of fungicide carbendazim in dilute aqueous solutions using nano TiO<sub>2</sub>

Taranjeet Kaur<sup>a</sup>, Amrit Pal Toor<sup>b,\*</sup>, Ravinder Kumar Wanchoo<sup>b</sup>

<sup>a</sup>Energy Research Center, Panjab University, Chandigarh, India

<sup>b</sup>Dr SSB University Institute of Chemical Engineering and Technology, Panjab University, Chandigarh, India

Tel. +9814173832; email: aptoor@yahoo.com

Received 26 July 2013; Accepted 17 December 2013

---

### ABSTRACT

The carbendazim is a widely used benzimidazole fungicide. It is of major concern due to its suspected hormone disrupting effects. The degradation of carbendazim considered as a “priority hazard substance” by the Water Framework Directive of the European Commission was investigated by UV/solar photocatalytic process using P25 TiO<sub>2</sub> and LR grade TiO<sub>2</sub>. A batch-type photoreactor was employed and the influence of catalyst loading, initial concentration, area/volume ratio, pH of the solution and light conditions were studied. Aeroxide P25 shows better degradation efficiency than LR grade TiO<sub>2</sub> in both UV and sunlight conditions for optimized parameters. Degradation of fungicide was negligible with TiO<sub>2</sub> under UV without catalyst. However, no adsorption took place with catalyst in dark. Also, the addition of oxidant (H<sub>2</sub>O<sub>2</sub>) had no appreciable increase in the rate of degradation for both the catalysts. Under UV light with TiO<sub>2</sub> carbendazim has shown substantial degradation at different time of irradiation. The optimized parameters under UV for the degradation of carbendazim are catalyst loading 1 g L<sup>-1</sup>, area/volume ratio 0.919 cm<sup>2</sup> ml<sup>-1</sup>, intensity 30 W m<sup>-2</sup>, pH 6.5 and around 85% mineralization of carbendazim was achieved.

*Keywords:* Photocatalytic degradation; Carbendazim (technical); TiO<sub>2</sub>; TiO<sub>2</sub> LR; Slurry reactor; H<sub>2</sub>O<sub>2</sub> and UV

---

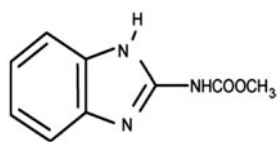
### 1. Introduction

Fungicides are either chemicals or biological agents that inhibit the growth of fungi or fungal spores. Fungi can cause serious damage in agriculture, resulting in critical losses of yield and quality [1]. The residues of fungicide have been detected on food grains that are used for human consumption mainly because of post harvest treatments of seeds [1].

Fungicides directly inhibit sterol synthesis in membrane and DNA synthesis [2]. Because of their chemical characteristics, fungicides represent a type of pollutant that shows variable persistence and photochemical degradation [3]. Out of them carbendazim is one of the concerned fungicide. The carbendazim [MBC (methyl-2-benzimidazole carbamate)] is a widely used systemic fungicide for controlling a broad range of fungi affecting fruits, nuts, vegetables, turf, and field crops. The structure of carbendazim is shown below:

---

\*Corresponding author.



Additionally, the carbendazim and n-butylisocyanate (BIC) are degradation products of benomyl fungicide (methyl-1-(butylcarbamoyl)-2-benzimidazole carbamate) in water and in organic solvents [4]. Systemic fungicides, benomyl, and carbendazim are toxic and can be adsorbed through the roots, leaves, and green tissues of flora along with water [5]. These products, benomyl, carbendazim and BIC, are harmful for humans, animals and plants. This toxicity includes effects in the male mammalian reproductive system, embryotoxicity, teratogenesis [6–8], and phytotoxicity [9,10]. The half-life of carbendazim on bare soil is 6–12 months and in water is around 2–25 d in aerobic and anaerobic conditions, respectively [11]. Therefore, the quantitative determination is very important for carbendazim in water, soil, wastewater, crops, and foods. Treatment of water by advanced oxidation processes (AOPs), that is useful for purifying drinking water and cleaning industrial wastewater, has been used extensively worldwide [12]. AOPs include photocatalysis systems which generate OH radical when a semiconductor ( $\text{TiO}_2$ , ZnO etc.) is excited by absorbing UV light equivalent to its band gap energy.  $\text{TiO}_2$  has been widely used because of its various merits such as low cost, nontoxicity, photocatalytic, and chemical activity.

Previously some researchers have studied the degradation of carbendazim using diverse methods. The photodecomposition of fungicide carbendazim has been studied in aqueous solution at several pH under different experimental conditions and found that at alkaline solution degradation was more rapid as compared to acidic solution [13–15]. The transformation of fungicide carbendazim by hydrogen peroxide has been studied in the absence and occurrence of carbonate ions. It was found that the presence of hydrogenocarbonate ions cause a quenching effect, which cause the degradation of carbendazim [16]. Work on synthetic and natural dye pigments as photosensitizers has also been investigated for the visible light photodegradation of the colorless solution of this fungicide [17]. Thermal adsorption and catalytic photodegradation of carbendazim in river water and soil has been studied and the effect of nitrite and nitrates ions was observed [18]. Xiao et al. [19] had studied the sonolytic ozonation of carbendazim with

the variation in pH with ozone dose. It was observed that sonolytic technique alone is not that efficient, but combination of ozonation and sonolysis can effectively degrade carbendazim, but higher concentration of ozone dose is required. The degradation of carbendazim have been studied by Rajeswari and co-workers using  $\text{TiO}_2$ ,  $\text{O}_3$ , and combination [20–22]. They have mainly studied the degradation on  $\text{O}_3$  using UV at 253 nm. Moreover, they have studied the degradation of commercial carbendazim using  $\text{TiO}_2$  and have achieved 76% degradation in one hour. Work on optimization, kinetics, and toxicity studies was also reported but with immersion type of reactor [23]. Such reactions are of high cost and these reactions are limited to small-scale applications. Our aim is to degrade fungicide economically under UV (365 nm) and solar light conditions by reducing the cost of catalyst.

In this paper, we have focused on the degradation of fungicide carbendazim in batch type of reactor. Different reaction parameters, such as concentration of catalyst, pH,  $A/V$ , different light intensity, and addition of oxidant  $\text{H}_2\text{O}_2$ , were investigated with both P25 and LR grade  $\text{TiO}_2$ . The photodegradation of carbendazim has also been studied under different light conditions i.e. UV and sunlight by keeping all other parameters optimum. Moreover, degradation of carbendazim with low price LR grade  $\text{TiO}_2$  was not reported in the literature as far as our knowledge is concerned. Thus, LR grade  $\text{TiO}_2$  was tested in order to reduce the operating cost of the system.

## 2. Materials and methods

Carbendazim (98.5%, technical grade) was used as model pesticide which was kindly provided by Markfed agro chemicals Mohali.  $\text{TiO}_2$  Aeroxide P25 (purity 97%, average particle size of 30 nm and anatase to rutile ratio was 80:20) bought from Aeroxide (China) industries was used as photocatalyst without any further preliminary treatment. LR grade  $\text{TiO}_2$  (Minimum assay 98.0%) was purchased from SD Fine-Chemicals, Mumbai.  $\text{H}_2\text{O}_2$  (assay 29–32%) was purchased from Merck, India. Membrane filters of 0.22  $\mu\text{m}$  (Millipore, from USA) were used to separate the  $\text{TiO}_2$  particles from the samples. All the aqueous solutions were prepared with double distilled water. A batch-type reactor set up with an artificial light was irradiated. A stock solution having 10  $\text{mg L}^{-1}$  carbendazim concentration was prepared and degradation was carried out with nano  $\text{TiO}_2$ . Acidic or alkaline media were obtained by addition of HCl LR or NaOH (assay 97% from SDFCL products) to the aqueous solutions containing the substrate. The setup consist of

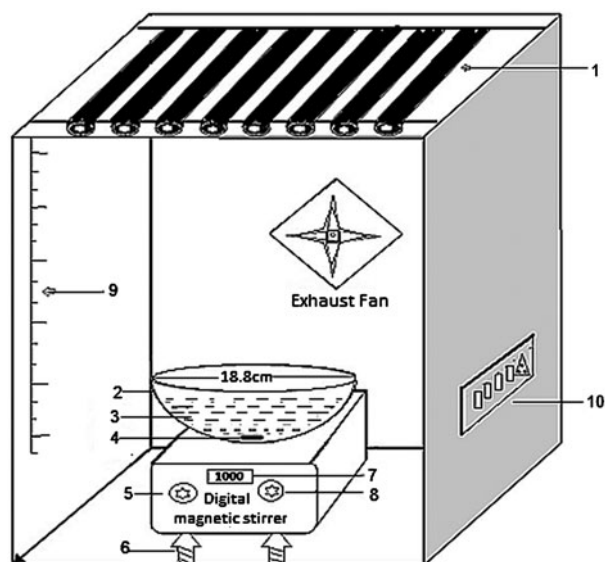


Fig. 1. Batch-type photocatalytic reactor setup. (1) Blue-black UV lamps (20 W), (2) hemispherical reactor vessel, (3) reaction solution, (4) magnetic bead, (5) RPM controller, (6) adjustable stand, (7) RPM display, (8) temperature controller, (9) scale, and (10) electric switch.

a UV chamber having  $70 \times 45 \times 75$  cm, consisting of  $8 \times 20$  W UV black florescent lamps (Philips) arranged in parallel inside the top of the chamber having wavelength 365 nm as shown in Fig. 1. Analysis of samples was done using Shimadzu UV-vis spectrophotometer.

### 3. Analyses

For all analytical purposes, Shimadzu UV-vis spectrophotometer (model no. 2450) was used. In order to perform the experiments, a solution containing  $10 \text{ mg L}^{-1}$  of carbendazim was initially prepared. The pH was adjusted to the desired value by means of a pH meter (Perfit India) using dilute HCl and NaOH solutions. Light intensity was measured using Solar Light Co. PMA2100, Intentiometer. The crystalline structure of both catalysts was determined by a Pan analytical X'Pert Pro diffractometer (D/max rA) at 45 kV and 40 mA ( $\text{Cu K}\alpha = 1.504060 \text{ \AA}$ ). Analysis was performed after separation of the photocatalyst particles by membrane filtration with a UV-vis spectrophotometer measuring the absorbance at wavelength ( $\lambda_{\text{max}}$ ) 285 nm. Also, the mineralization of carbendazim was observed by COD Vario photometer (RD 125), Orbit India.

## 4. Results and discussion

### 4.1. Absorption spectra

Degradation of carbendazim using  $\text{TiO}_2$  photocatalyst was studied and the samples withdrawn at regular

interval of time were observed using UV-vis spectroscopy. The absorption spectra of carbendazim showed a strong distinctive peak at wavelength 285 nm. The gradual decrease in the peak intensity was observed with the decrease in the fungicide concentration. As discussed by Saien et al. the peak at 285 nm accredited to benzene ring which can be attacked by hydroxyl radicals [23–25]. The important fragment in these reactions is aryl radical group which can be decomposed after radicalizing [26]. Therefore, it is entrenched that the degradation of carbendazim occurred at different intervals of time as shown in Fig. 2. After 60 min, the peak is completely vanished in the presence of  $\text{TiO}_2$  suspension.

### 4.2. Photodegradation reactions

Carbendazim solution was irradiated with a known amount of nano  $\text{TiO}_2$  catalyst. As shown in Fig. 3, adsorption was negligible with  $\text{TiO}_2$  under dark and hence no adsorption takes place on the surface of catalyst. Also, UV light alone cannot degrade fungicide in the absence of catalyst. The degradation of carbendazim takes place in around 60 min under UV/ $\text{TiO}_2$ .

The photocatalytic oxidation of carbendazim in water has been successfully modeled using Langmuir-Hinshelwood kinetics. According to the Langmuir-Hinshelwood model:

$$-\frac{dC}{dt} = \frac{k'KC}{1 + KC} \quad (1)$$

where  $C$  is the bulk concentration,  $k'$  is reaction rate constant,  $K$  is equilibrium adsorption constant and  $t$  represents time. For low solute concentration  $KC$  is

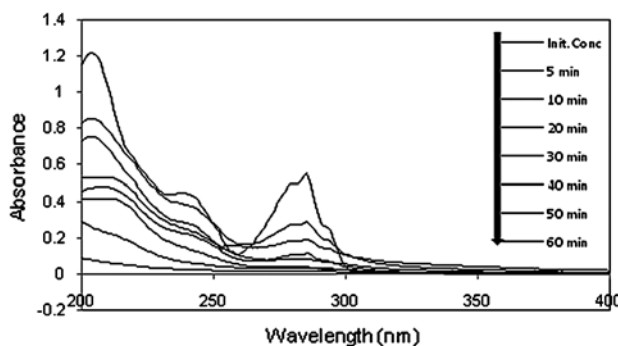


Fig. 2. Absorption spectra changes for degradation of carbendazim with  $\text{TiO}_2$  under UV light (carbendazim  $10 \text{ mg L}^{-1}$ , pH 6.5, UV  $30 \text{ W m}^{-2}$ , and  $\text{P}25 \text{ 1 g L}^{-1}$ ).

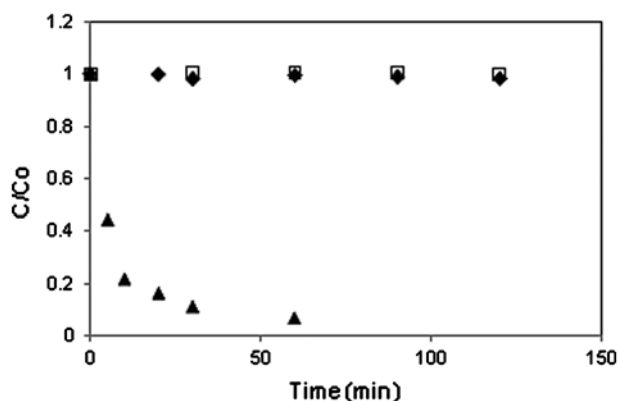


Fig. 3. Photocatalytic degradation (◆) reaction in dark, (■) UV without TiO<sub>2</sub> (▲) UV with TiO<sub>2</sub>. (carbendazim 10 mg L<sup>-1</sup>, pH 6.5, P25 1 g L<sup>-1</sup>).

usually much smaller than one. This reduces the above equation to pseudo first order equation:

$$\ln(C_0/C) = kt \quad (2)$$

where  $C_0$  is the initial concentration and  $k$  is apparent rate constant. Plot of  $\ln(C_0/C)$  gives a straight line which shows that it obeys pseudo-first-order kinetics.

Due to the character of photocatalytic reaction,  $k$  is a function of parameters such as UV light intensity, catalyst loading, pH of the solution, addition of the oxidant (H<sub>2</sub>O<sub>2</sub>), and initial concentration of pollutant and geometry of the photoreactor.

#### 4.3. Degradation of carbendazim with different amount of aeroxide P25

A series of experiments were carried out to assess optimum catalyst dosage by varying the amount of TiO<sub>2</sub> (0–2.5 g L<sup>-1</sup>) for degradation of carbendazim (10 mg L<sup>-1</sup>). Degradation increases with increase in TiO<sub>2</sub> dosage up to 1.0 g L<sup>-1</sup>, after which there was gradual decrease in degradation rate, as shown in Fig. 4. The rate constant versus catalyst loading is shown in Fig. 5. The figure shows that optimum catalyst loading for maximum degradation was achieved with 1 g L<sup>-1</sup> TiO<sub>2</sub>. In carbendazim, initial increase in degradation with increase in catalyst dosage was observed due to increase in number of active sites, hydroxyl radical generation, surface area, and light absorption. Decrease above 1 g L<sup>-1</sup> TiO<sub>2</sub> was attributed due to scattering of light by increased opacity of suspension and decline in number of active sites [24]. Also increase in catalyst dosage above optimum level resulted in decrease in light penetration and causes

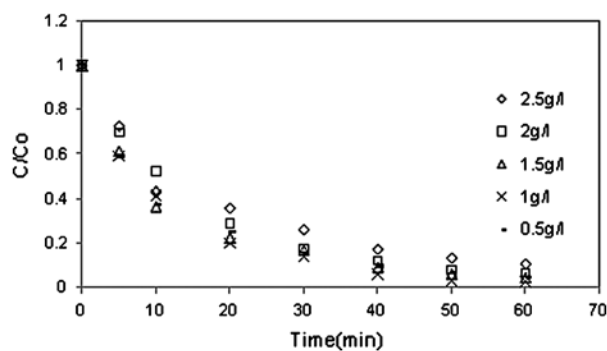


Fig. 4. Effect of catalyst loading on the degradation of carbendazim (carbendazim 10 mg L<sup>-1</sup>, pH 6.5, 30 Wm<sup>-2</sup>).

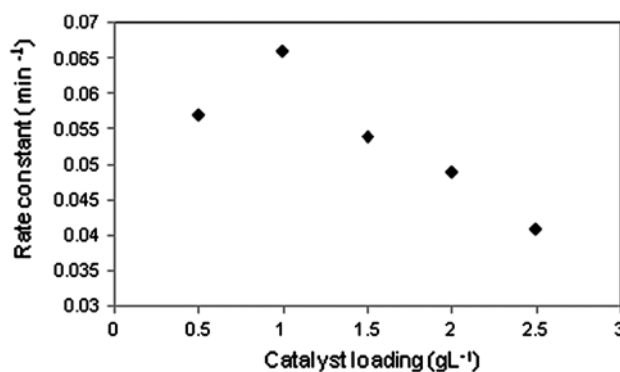


Fig. 5. Plot of rate constant vs. catalyst loading on carbendazim degradation (carbendazim 10 mg L<sup>-1</sup>, pH 6.5, 30 Wm<sup>-2</sup>).

deactivation of activated molecules due to collision with ground-state molecule [27]. The aggregation of particles may also reduce effectual surface area of catalyst for adsorption of reactant [28].

#### 4.4. Effect of pH

The amphoteric behavior of titania influences the surface charge of the photocatalyst. The role of pH on the photocatalytic degradation of carbendazim was studied in the pH range 1–9 at constant carbendazim concentration of 10 mg L<sup>-1</sup> and catalyst dose 1 g L<sup>-1</sup> [29]. The natural pH of carbendazim solution (6.3) shows maximum results as compared to the other pH values, since pH 1 and 3 are significantly less than the pK<sub>a</sub> (=4.5) of carbendazim in aqueous solution [14]. At lower pH, protonation of carbendazim takes place and the protonated groups are more stable under UV radiation than its main structure [30]. The zero point charge, pH<sub>ZPC</sub>, for titania is around 6.8 and in acidic pH it is positively charged and in alkaline pH it is

negatively charged, and thus catalyst surface is also positively charged leading to a lower level of degradation at pH 1 and 3 [31]. Thus, the acceptance of electron by the dissolved oxygen decreases the recombination of valance band hole and conduction band electron. Similarly, at pH 9 rate of degradation is not as much as observed at natural pH, as shown in Fig. 6.

#### 4.5. Effect of initial concentration

Initial concentrations of reactants play a significant role in determining the rates of most of chemicals and photochemical reactions. This was evident in the degradation patterns for the fungicides given in Fig. 7. The degradation rate for carbendazim in the initial stages was faster, followed by relatively slower removal efficiency at later stages. There was reduction in the rate and extent of degradation of carbendazim as the initial concentration was increased from 5 to 12 mgL<sup>-1</sup>. At higher fungicide's concentrations, there would be more adsorption of fungicides on TiO<sub>2</sub> resulting in a lesser availability of catalyst surface for hydroxyl radical generation. The rate of degradation depends upon the formation of hydroxyl radicals, which has critical role in the degradation process [32,33]. With the increase in concentration of pesticide the screening effect dominates and prevent the penetration of the light [34].

#### 4.6. Effect of area/volume ratio of the reactor

In shallow-pond batch-type reactor, depth of solution is an important parameter as penetration of light decreases with increase in depth and more the area, more will be penetration of light on the surface. If the surface area of the solution is increased the path

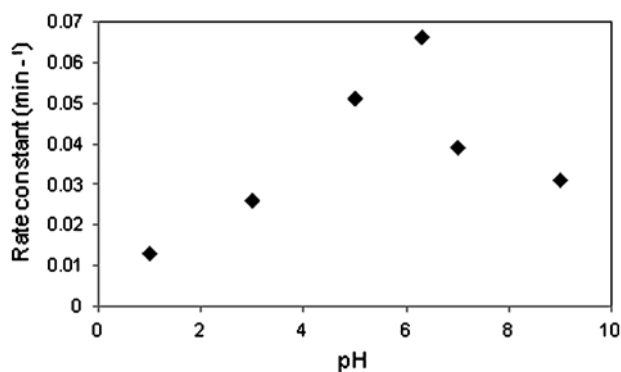


Fig. 6. Plot between rate constant vs. pH of carbendazim (carbendazim 10 mg L<sup>-1</sup>, 30 Wm<sup>-2</sup>, P25 1 g L<sup>-1</sup>).

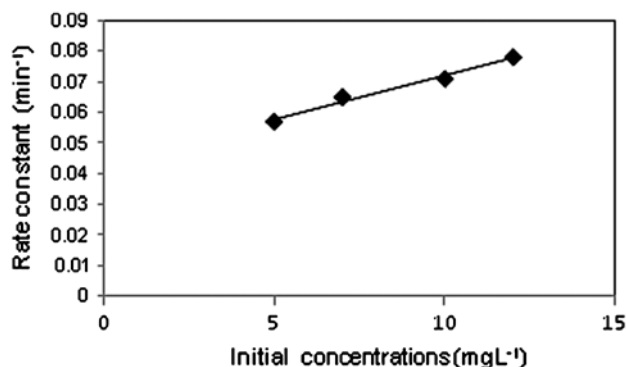


Fig. 7. Effect of initial concentration on degradation rate with time on carbendazim (pH 6.5, 30 Wm<sup>-2</sup>, P25 1 g L<sup>-1</sup>).

length of photons entering the solution increases hence the formation of OH radical increases. More area and less depth enhance the rate of degradation as the penetration of UV rays increases [35]. Hence, the reaction rate constant increases with increasing area to volume ratio as shown in Fig. 8. As the A/V ratio increases from 0.575 to 1.324 cm<sup>2</sup> ml<sup>-1</sup>, the degradation rate constant increases from 0.048 to 0.072 min<sup>-1</sup>. After irradiation for one hour, it was observed that the solution with highest A/V ratio shows maximum degradation under UV light i.e. about 96.0%, whereas the lowest degradation was found in the solution having maximum initial volume. But its A/V ratios of 0.919 cm<sup>2</sup> ml<sup>-1</sup> were used in all the reactions.

#### 4.7. Effect of light intensity

The reaction rate constant varies with the intensity of incident light and the type of reactor used. For shallow-pond batch reactor, the intensity dependence of the reaction rate constant is given by:

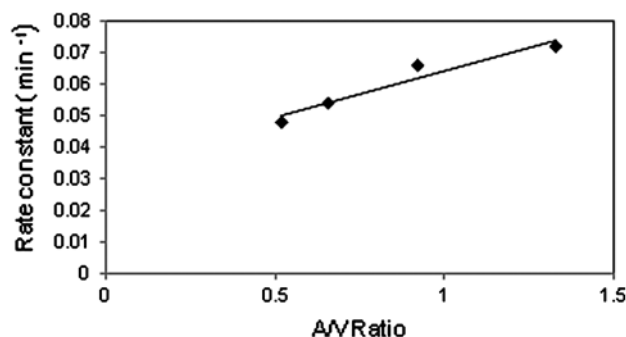


Fig. 8. Degradation of carbendazim at different A/V ratios of the reactor (carbendazim 10 mg L<sup>-1</sup>, pH 6.5, 30 Wm<sup>-2</sup>, P25 1 g L<sup>-1</sup>).

$$\frac{k}{k_0} = m \left[ \frac{I(A/V)}{I_0(A/V)_0} \right]^n \quad (3)$$

where  $m$  and  $n$  are the empirical constants whose values have reported by Wyness et al. [35] for some systems and  $k_0$  is reference rate constant corresponding to reference intensity  $I_0$ . Hence, the constant  $k$  is dependent on the intensity when the aperture to volume ratio ( $A/V$ ) is kept constant as shown in Eq. (2).

$$\frac{k}{k_0} = m \left[ \frac{I}{I_0} \right]^n \quad (4)$$

To study the effect of intensity, the aperture to volume ratio ( $A/V$ ) was kept constant at  $0.919 \text{ cm}^2 \text{ ml}^{-1}$  and intensity was varied from 20 to  $35 \text{ Wm}^{-2}$ . The value of degradation rate constant increased from  $0.515$  to  $1.327 \text{ min}^{-1}$  as intensity increases from 20 to  $35 \text{ Wm}^{-2}$ . Fig. 9 shows the relation between reaction rate constant  $k$  and intensity for constant  $A/V$  ratio. The value of  $n$  is 0.796 and  $m$  is 0.998 as calculated from Fig. 9. These values are quite similar with the value reported in 3,4-dichlorophenol in shallow pond batch reactor [35,36].

#### 4.8. Degradation with $\text{TiO}_2$ LR grade

$\text{P25 TiO}_2$  is a very efficient catalyst under UV but it is expensive. To reduce the cost of  $\text{TiO}_2$ , LR grade which is easily available in the local market was studied. It is used for the degradation of carbendazim in slurry mode and showed quite satisfactory results. To compare this catalyst with P25, the degradation

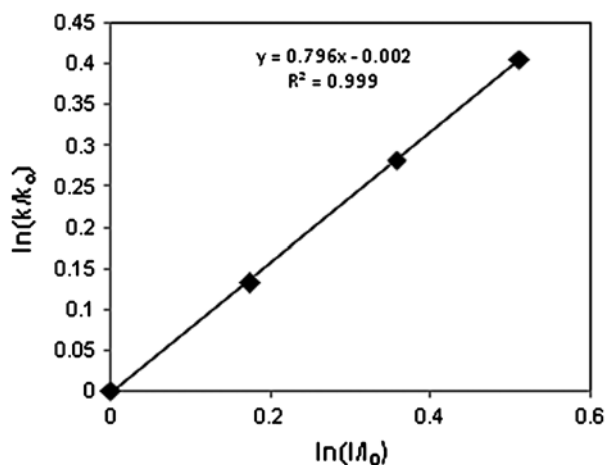


Fig. 9. Rate constant variation with UV intensity (carbendazim  $10 \text{ mg L}^{-1}$ , pH 6.5,  $\text{P25 } 1 \text{ g L}^{-1}$ ).

studies with  $\text{TiO}_2$  LR was done by varying the catalyst dosage at optimum conditions. The optimum catalyst loading of  $\text{TiO}_2$  LR is also found to be  $1 \text{ g L}^{-1}$ , as shown in Fig. 10.

#### 4.9. Comparison of P25 with $\text{TiO}_2$ LR grade

The effect on degradation of carbendazim was investigated by treating the aqueous solution in both UV and sunlight conditions using P25 and  $\text{TiO}_2$  LR. Fungicide carbendazim was effectively degraded by  $\text{TiO}_2$  LR. As Aeroxide P25 has smaller particle size and higher purity than LR grade  $\text{TiO}_2$ , thus it shows better degradation under both light (UV and sunlight) conditions as shown in Fig. 11(a) and (b). The percentage degradation of carbendazim in UV light with P25 was 96% and  $\text{TiO}_2$  LR was 94% under similar conditions with catalyst concentration  $1 \text{ g L}^{-1}$ , pH 6.3, initial concentration  $10 \text{ mg L}^{-1}$ , and light intensity  $30 \text{ Wm}^{-2}$ . Degradation under sunlight (SL) was also investigated with both catalysts and found that both catalysts show less degradation as compared to that under UV light and the efficiency of  $\text{TiO}_2$  LR is slightly less than P25 as shown in Fig. 12.

The decrease in the efficiency of  $\text{TiO}_2$  LR grade as compared to P25 can be supported by results of XRD of both the samples as shown in Fig. 13(a) and (b). It is noted that the XRD peaks of  $\text{TiO}_2$  LR and P25 have the same positions by the height. P25 at  $2\theta = 27.5^\circ$ , preferably showing the presence of rutile phase whereas the anatase and rutile could not be detected in  $\text{TiO}_2$  LR grade [37]. Moreover, it could be seen that the P25 has lower intensity than  $\text{TiO}_2$  LR at 1,300 and 6,000, respectively. It was observed that P25 has wider peak than  $\text{TiO}_2$  LR at  $2\theta = 25.3^\circ$ , which implies that

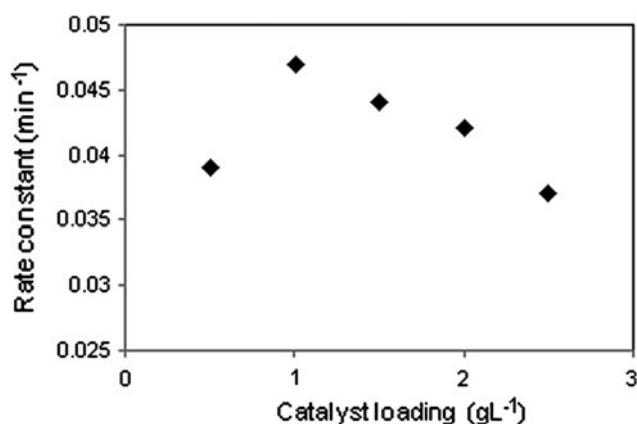


Fig. 10. Plot showing rate constant vs. catalyst loading of  $\text{TiO}_2$  LR on carbendazim (carbendazim  $10 \text{ mg L}^{-1}$ , pH 6.5, and UV  $30 \text{ Wm}^{-2}$ ).

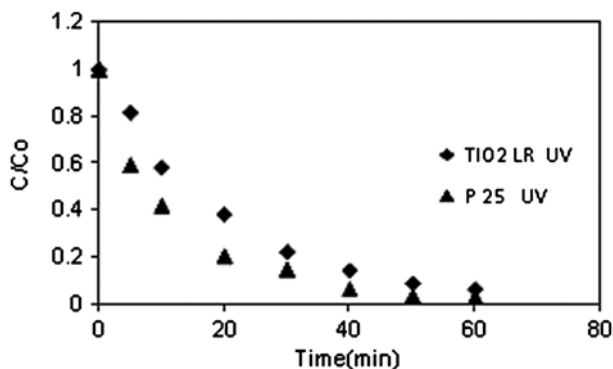


Fig. 11. (a) Comparison plot for the degradation of carbendazim with P25 and TiO<sub>2</sub> LR under UV light (carbendazim 10 mg L<sup>-1</sup>, pH 6.5, UV 30 Wm<sup>-2</sup>).

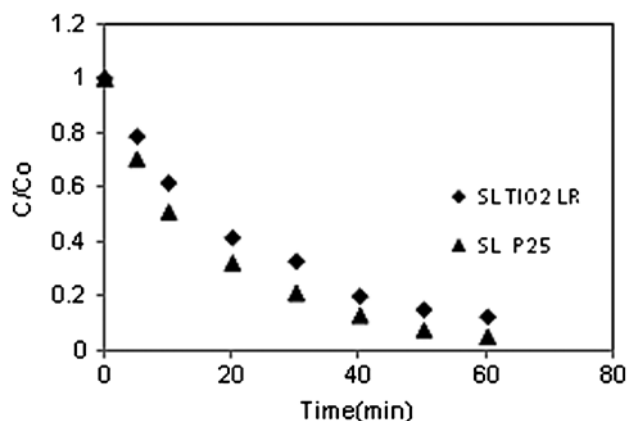


Fig. 11. (b) Comparison plot for the degradation of carbendazim with P25 and TiO<sub>2</sub> LR in sunlight (carbendazim 10 mg L<sup>-1</sup>, pH 6.5, 35 Wm<sup>-2</sup>).

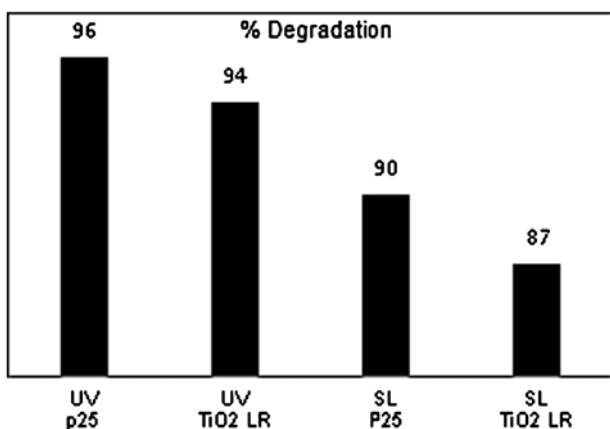


Fig. 12. Percentage degradation of carbendazim with both catalysts in UV and sunlight (carbendazim 10 mg L<sup>-1</sup>, pH 6.5, P25 & LR 1 g L<sup>-1</sup>).

P25 has smaller grain size and spherical shape, and therefore provide large surface area comparatively. Large crystallites give rise to sharp peaks, which increase the peak width as the decrease in the crystallite size. The crystalline size represents specific surface area (m<sup>2</sup> g<sup>-1</sup>) of catalyst which affects its photoactivity. A small crystalline size has higher specific area than the larger crystallite [38]. As the surface area increases the light received per unit area also increases; and hence leads to more electronic excitations, thus increases the photoefficiency of the catalyst, which can be the major reason for better performance of P25 TiO<sub>2</sub> as compared to LR grade TiO<sub>2</sub>.

Determination of crystal size of P25 and TiO<sub>2</sub> LR was done using Scherer equation:

$$D = K\lambda/\beta \cos \theta \quad (5)$$

where  $D$  is the crystal grain size,  $K$  is dimensionless constant (0.9),  $\theta$  is the X-ray diffraction angle,  $\lambda$  is wavelength of X-ray radiation (0.15418 nm), and  $\beta$  is the full width at half maximum of diffraction peak. Hence, calculated crystallite size for P25 TiO<sub>2</sub> and TiO<sub>2</sub> LR was 32.8 and 59.5 nm, respectively.

Diffuse reflectance spectra is an excellent diagnostic tool in which powdered, crystalline, and nanostructure materials at different spectral ranges i.e. 200–700 nm are studied. Diffuse reflectance spectroscopy studies for P25 TiO<sub>2</sub> and TiO<sub>2</sub> LR samples are shown in Fig. 14. It shows that  $\lambda_{\max}$  decreases in case of TiO<sub>2</sub> LR. This increase in band gap of LR TiO<sub>2</sub> predicts that more energy is required for formation of electron hole. Hence, decrease in band gap can be another reason for the enhanced results of P25 as compared to LR grade TiO<sub>2</sub>.

#### 4.10. Addition of oxidant

In order to enhance the photocatalytic degradation rate of carbendazim under UV light and sunlight, an oxidant (H<sub>2</sub>O<sub>2</sub>) is added into a semiconductor suspension in both P25 Aeroxide and TiO<sub>2</sub> LR grade. The effect of H<sub>2</sub>O<sub>2</sub> has been investigated in numerous studies and it was observed that it increases the degradation rate of organic pollutants [39]. But in our case, addition of oxidant H<sub>2</sub>O<sub>2</sub> has no appreciable increase in the rate of degradation under UV light as shown in Fig. 15. The observed trend can be explained by the fact that the addition of oxidants enhances the degradation rate only if there is a scarcity of oxygen species in the reaction solution [40]. Also, because H<sub>2</sub>O<sub>2</sub> is activated in acidic conditions and we are working at nearly neutral pH so this can be a another reason for the low activity of H<sub>2</sub>O<sub>2</sub> [41].

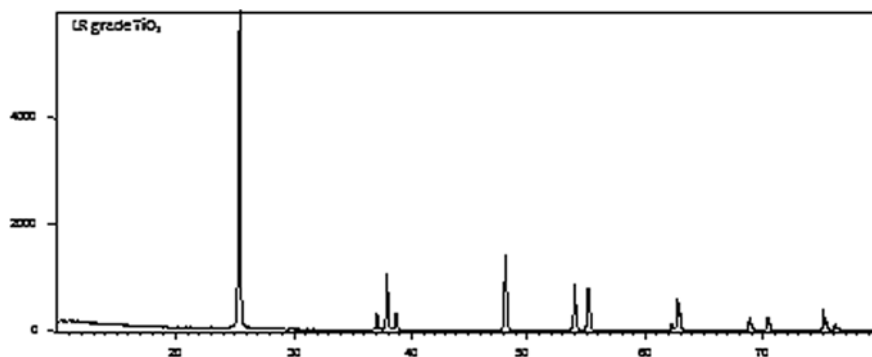


Fig. 13. (a) Graph of XRD of TiO<sub>2</sub> LR.

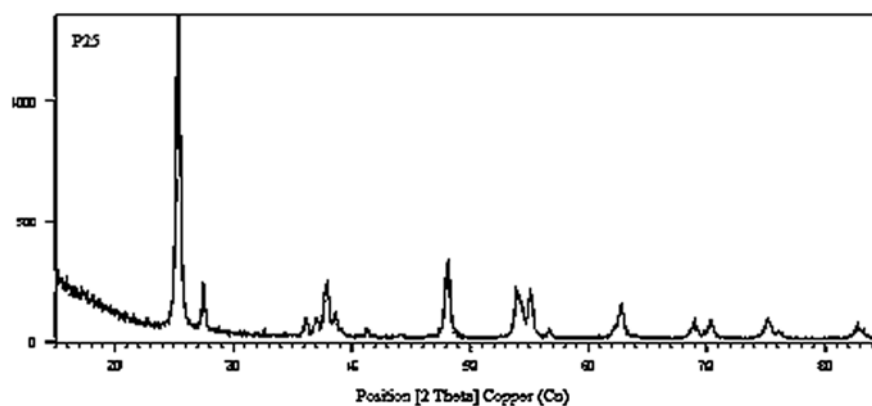


Fig. 13. (b) Graph of XRD of P25.

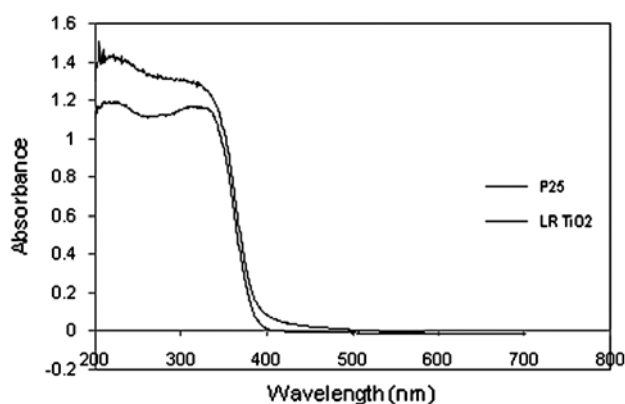


Fig. 14. Graph showing UV–vis diffuse spectra of P25 and TiO<sub>2</sub> LR (carbendazim 10 mg L<sup>-1</sup>, pH 6.5, UV 30 Wm<sup>-2</sup>).

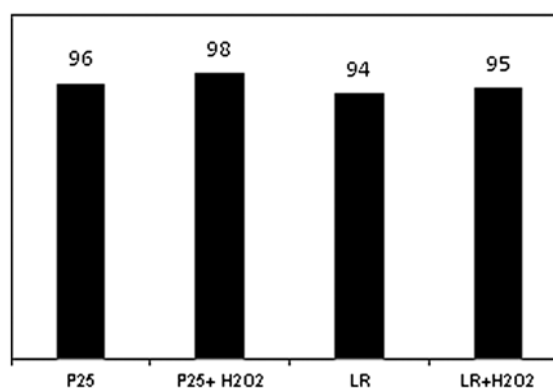


Fig. 15. Percentage degradation of carbendazim using P25 and LR grade TiO<sub>2</sub> alone and with addition of oxidant H<sub>2</sub>O<sub>2</sub> (carbendazim 10 mg L<sup>-1</sup>, pH 6.5, UV 30 Wm<sup>-2</sup>).

### 5. Mineralization of carbendazim

The reduction of COD reflects the extent of mineralization of an organic species. Therefore, the change in COD was studied for carbendazim under optimized conditions as a function of irradiation time under UV as well as sunlight. Fig. 16(a) and (b) shows

change in concentration and % COD removal as a function of time at optimum conditions. The figure shows that this process is not only degrading the carbendazim but also mineralizing the synthetic effluents. Under optimum conditions fungicide showed 85% mineralization in UV and 80% in sunlight.

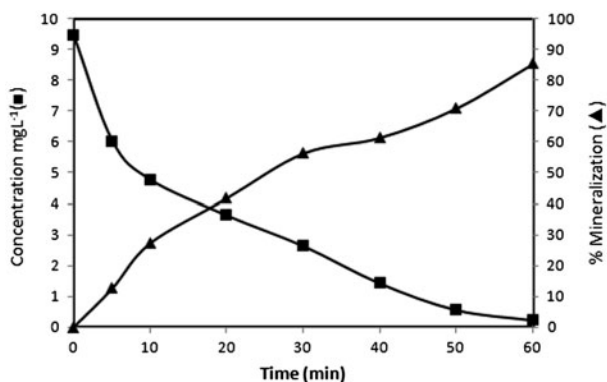


Fig. 16. (a) Plot showing COD removal for carbendazim under UV (carbendazim  $10 \text{ mg L}^{-1}$ , pH 6.5, UV  $30 \text{ Wm}^{-2}$ , P25  $1 \text{ g L}^{-1}$ ).

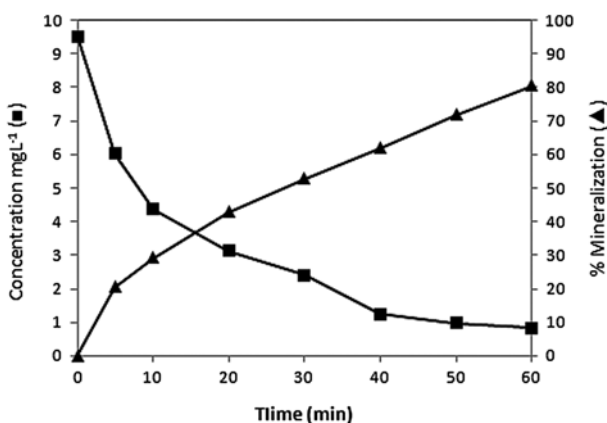


Fig. 16. (b) Plot showing COD removal for carbendazim under sunlight (carbendazim  $10 \text{ mg L}^{-1}$ , pH 6.5, and P25  $1 \text{ g L}^{-1}$ ).

## 6. Conclusions

Effective photocatalytic degradation of the fungicide carbendazim is possible using P25 and  $\text{TiO}_2$  LR catalyst in suspended aqueous solutions under UV light and sunlight irradiation. Study of  $\text{TiO}_2$  LR grade for the degradation of carbendazim has a fruitful role but less effective as compared to P25. The adsorption of substrate on the catalyst particles was negligible during photocatalytic degradation. The degradation rate increases with increase in catalyst loading (P25 and  $\text{TiO}_2$  LR grade) up to  $1 \text{ g L}^{-1}$  at pH 6.3, initial concentration  $10 \text{ mg L}^{-1}$ , light intensity  $30 \text{ Wm}^{-2}$  and  $A/V$  ratio  $0.919 \text{ cm}^2 \text{ ml}^{-1}$ . With optimum catalyst loading the degradation of carbendazim takes place in around 60 min with both the catalysts. Addition of oxidant ( $\text{H}_2\text{O}_2$ ) with P25 and  $\text{TiO}_2$  LR was studied and not much appreciable increase in degradation was

observed both in UV light and under sunlight. Carbendazim shows effective mineralization under UV and sunlight in 60 min with P25 and  $\text{TiO}_2$  LR.

## List of symbols

$k'$	—	reaction rate constant
$k$	—	equilibrium adsorption constant
$C$	—	bulk constant
$C_0$	—	initial concentration
$k$	—	apparent rate constant
$m, n$	—	empirical rate constant
$k_0$	—	reference rate constant
$I_0$	—	reference intensity
$I$	—	intensity of incident light
$D$	—	constant grain size
$K$	—	dimensionless constant
$Q$	—	full width at half maximum (FWHM)

## References

- [1] R. Rouabhi, Fungicides, IN Tech Publications, Algeria, 2010, pp. 363–382.
- [2] G.T. Brooks, T.R. Roberts, Pesticide Chemistry and Bioscience, Special Publications, Algeria, 1999.
- [3] E.R. Bandala, S. Gelover, M.T. Leal, C.A. Bulnes, A. Jimenez, C.A. Estrada, Solar photocatalytic degradation of Aldrin, J. Catal. Today 76(2–4) (2007) 189–199.
- [4] S.M. Arnold, R.E. Talaat, W.J. Hickey, R.F. Harris, Identification of Fenton's reagent-generated atrazine degradation products by high-performance liquid chromatography and megafLOW electrospray ionization tandem mass spectrometry, J. Mass Spectro. 30(3) (1995) 452–460.
- [5] A. Ben-Aziz, N. Aharanson, Dynamics of uptake translocation, and disappearance of thiabendazole and methyl-2 benzimidazole carbamate in pepper and tomato plants, J. Pest. Biochem. Physiol. 4 (1976) 120–126.
- [6] M.E. Axness, J.R. Flecker, Metabolism of the butylcarbamoyl moiety of benomyl in rat, Pest. Biochem. Physiol. 11 (1972) 1–12.
- [7] R.A. Hess, B.J. Moore, J. Forrer, R.E. Linder, A.A. Abuel-Atta, The fungicide benomyl causes testicular dysfunction by inducing the sloughing of germ cells and occlusion of efferent ductless, J. Fundam. App. Toxicol. 47 (1994) 1197–1206.
- [8] L. Somerville, The metabolism of fungicides, J. Xenobiot. 16 (1986) 1017–1030.
- [9] D.G. Shilling, H.A. Moyer, H.C. Aldrich, J.E. Gauder, M. Buszko, J.P. Toth, W.S. Brey, B. Bechtel, J.K. Tolson, N,N dibutylurea from n-butylisocyanate, a degradation product of benomyl: Formation in benlate formulations and on plants, J. Agric. Food Chem. 42 (1994a) 1204–1208.
- [10] D.G. Shilling, H.C. Aldrich, H.A. Moyer, J.F. Gaffney, J.K. Tolson, R. Querns, M.A. Mossler, N,N'-dibutylurea from n-butyl isocyanate, a degradation product of benomyl. 2. Effects on plant growth and physiology, J. Agric. Food Chem. 42 (1994b) 1209–1212.

- [11] Pesticides residues in food-1997 evaluations, Part I Residues, FAO Plant production and protection paper, Rome (1998), p. 146.
- [12] G. Zelmanov, R. Semiat, Iron(3) oxide-based nanoparticles as catalysts in advanced organic aqueous oxidation, *Water Res.* 42 (2008) 492–498.
- [13] A. Boudina, C. Emmelin, A. Baaliouamer, M.F. Grenier-Loustalot, J.M. Chovelon, Photochemical behaviour of carbendazim in aqueous solution, *Chemosphere* 50 (2003) 649–655.
- [14] P. Mazellier, Émilie Leroy, B. Legube, Photochemical behavior of the fungicide carbendazim in dilute aqueous solution, *J. Photochem. Photobiol. A* 153 (2002) 221–227.
- [15] R. Panadés, A. Ibarz, S. Esplugas, Photodecomposition of carbendazim in aqueous solutions, *Water Res.* 34 (2000) 2951–2954.
- [16] P. Mazellier, E. Leroy, J.D. Laat, B. Legube, Transformation of carbendazim induced by the H<sub>2</sub>O<sub>2</sub>/UV system in the presence of hydrogenocarbonate ions: Involvement of the carbonate radical, *New J. Chem.* 26 (2002) 1784–1790.
- [17] J.P. Escalada, A. Pajares, J. Gianotti, W.A. Massad, S. Bertolotti, F. Amat-Guerri, N.A. García, Dye-sensitized photodegradation of the fungicide carbendazim and related benzimidazoles, *Chemosphere* 65 (2006) 237–244.
- [18] S.G. Muhamad, K.M. Shareef, H.A. Smail, Thermal adsorption and catalytic photodegradation studies of carbendazim fungicide in natural soil and water, *Int. J. Chem.* 3(2) (2011) 218–226.
- [19] Z. Xiao, M. Wang, R. Lu Jian, Degradation of fungicide carbendazim in aqueous solution by sonolytic Ozonation, *IEEE*, (2011) 8166–8169.
- [20] R. Rajeswari, S. Kanmani, A study on degradation of pesticides waste water by TiO<sub>2</sub> photocatalysis, *J. Sci. Indus. Res.* 157 (2009) 269–276.
- [21] R. Rajeswari, S. Kanmani, TiO<sub>2</sub>-based heterogenous photocatalytic treatment combined with Ozonation for Carbendazim degradation, *Iran J. Environ. Health Sci. Eng.* 6 (2009) 61–66.
- [22] R. Rajeswari, S. Kanmani, Comparative study on photocatalytic oxidation and photolytic ozonation for the degradation of pesticide wastewaters, *Desalin. Water Treat.* 19 (2010) 301–306.
- [23] J. Saien, S. Khezrianjoo, Degradation of the fungicide carbendazim in aqueous solutions with UV/TiO<sub>2</sub> process: Optimization, kinetics and toxicity studies, *J. Hazard. Mater.* 157 (2008) 269–276.
- [24] D.L. Pavia, G.M. Lampman, D.L. Kriz, Introduction to Spectroscopy: A Guide for Students, 3rd ed., Saunders College Publications, London, 2000.
- [25] S. Chiron, A. Fernandez-Alba, A. Rodriguez, E. Garciaalvo, Pesticide chemical oxidation: state-of-the-art, *Water Res.* 34 (2000) 366–377.
- [26] F.A. Carey, R.J. Sundberg, Advanced Organic Chemistry, 4th ed., Kluwer Academic, New York, NY, 2002.
- [27] M.V. Shankar, B. Neppolian, S. Sakthivel, B. Arabin-doo, M.P. Palanichamy, V. Murugesan, Kinetics of photocatalytic degradation of textile dye reactive red 2, *Ind. J. Eng. Mater. Sci.* 8 (2001) 104.
- [28] R.J. Davis, K.A. Gainer, G.O. Neal, I. Wenwu, Photocatalytic decolourisation of wastewater dyes, *Water Environ. Res.* 66 (1995) 50–53.
- [29] K. Sivagami, R. Ravi Krishna, T. Swaminathan, Studies on photocatalytic degradation of monocrotophos in an annular slurry reactor using factorial design of experiments, *Water Sustain.* 1 (2011) 75–84.
- [30] J. Fernández, J. Kiwi, C. Lizama, J. Freer, J. Baeza, H.D. Mansilla, Factorial experimental design of Orange II photocatalytic discoloration, *J. Photochem. Photobiol. A* 151 (2002) 213–219.
- [31] Y. Chen, Z. Sun, Y. Yang, Q. Ke, Heterogeneous photocatalytic oxidation of polyvinyl alcohol in water, *J. Photochem. Photobiol. A* 142 (2001) 85–89.
- [32] M.V. Shankar, Enhanced photocatalytic activity for the destruction of monocrotophos pesticide by TiO<sub>2</sub>/H<sub>2</sub>, *J. Mol. Catal. A: Chem.* 223 (2004) 195–200.
- [33] A.P. Toor, V. Singh, J.K. Chand, P.K. Bajpai, A. Verma, Treatment of bleaching effluents from the pulp and the paper industry by photocatalytic oxidation, *J. Tappi.* 6(9) (2007) 9–13.
- [34] B.K. Avasarala, S.R. Tirukkovalluri, S. Bojja, Photocatalytic degradation of monocrotophos pesticide—An endocrine disruptor by magnesium doped titania, *J. Hazard. Mater.* 186 (2011) 1234–1240.
- [35] P. Wyness, J.F. Klausner, D.Y. Goswami, K.S. Schanze, Performance of non concentrating solar photocatalytic oxidation reactors, Part 1: Flate plate configuration, *J. Sol. Energy Eng.* 8 (1994) 116.
- [36] A.P. Toor, A. Verma, J.K. Chand, P.K. Bajpai, V. Singh, Photocatalytic degradation of 3,4-dichlorophenol using TiO<sub>2</sub> in a shallow pond slurry reactor, *Ind. J. Chem. Technol.* 12 (2005) 75–81.
- [37] S.A. Md Ali, A.Z. Abdullah, Sonocatalytic degradation of methyl orange dye in aqueous effluents, *IPCBE* 12 (2011) 296–302.
- [38] A.P. Toor, N. Yadav, R.K. Wanchoo, *Material Science Forum*. Trans Tech Publications, Zurich, 2013, pp. 271–284.
- [39] M. Halmann, Photodegradation of di-n-butyl-orthophthalate in aqueous solutions, *J. Photochem. Photobiol. A* 66 (1992) 215–223.
- [40] D.D. Dionysiou, M.T. Suidan, I. Baudin, J.M. Lainé, Effect of hydrogen peroxide on the destruction of organic contaminants-synergism and inhibition in a continuous-mode photocatalytic reactor, *Appl. Catal., B* 50 (2004) 259–269.
- [41] W. Chu, W.K. Choy, The effect of solution pH and peroxide in the TiO<sub>2</sub>-induced photocatalysis of chlorinated aniline, *J. Hazard. Mater.* 141 (2007) 86–91.